Enhancing Phase Mapping for High-throughput X-ray Diffraction Experiments using Fuzzy Clustering

Dipendra Jha[1,*], K. V. L. V. Narayanachari[2,*], Ruifeng Zhang[2], Denis T. Keane[3], Wei-keng Liao[1], Alok Choudhary[1], Yip-Wah Chung[2], Michael J. Bedzyk[2] and Ankit Agrawal[1]

[1]*Department of Electrical and Computer Engineering, Northwestern University, Evanston, IL, U.S.A.*

[2]*Department of Materials Science and Engineering, Northwestern University, Evanston, IL, U.S.A.*

[3]*DND-CAT Synchrotron Research Center, Northwestern University, Evanston, IL, U.S.A.*

Keywords: X-ray Diffraction, Phase Clustering, Unsupervised Learning, Fuzzy C-means Clustering, Hierarchical Clustering, Composition-phase Diagram, Fuzzy Representation.

Abstract: X-ray diffraction (XRD) is a widely used experiment in materials science to understand the composition-structure-property relationships of materials for designing and discovering new materials. A key aspect of XRD analysis is that the composition-phase diagram is composed of not only pure phases but also their mixed phases. Hard clustering approach treats the mixed phases as separate independent clusters from their constituent pure phases, hence, resulting in incorrect phase diagrams which complicate the next steps. Here, we present a novel clustering approach of XRD patterns by leveraging a fuzzy clustering technique that can significantly enhance the potential phase mapping and reduce the manual efforts involved in XRD analysis. The proposed approach first generates an initial composition-phase diagram and initial pure phase representations by applying the fuzzy c-means clustering algorithm, followed by hierarchical clustering to accomplish effortless manual merging of similar initial pure phases to generate the final composition-phase diagram. The proposed method is evaluated on the XRD samples from two high-throughput composition-spread experiments of Co-Ni-Ta and Co-Ti-Ta ternary alloy systems. Our results demonstrate significant improvement compared to hard clustering and almost completely eliminate manual efforts.

1 INTRODUCTION

High-throughput X-ray diffraction (XRD) experiments are a well-known technique used by materials scientists for characterizing the materials structure for understanding the composition-structure-property relationships of materials. The analysis of XRD patterns from high throughput experiments provides atomic-scale crystal structure details that are not only be used to predict the properties of materials (Woolfson and Woolfson, 1997; Klug and Alexander, 1974; Moore and Reynolds, 1989; Bish and Post, 1989; Cullity, 1978) , but are also used to determine the possible flaws in a material sample for novel materials design (Chung and Ice, 1999). High-throughput measurements combined with machine learning can improve the design process of the Co-super alloys.

[*]Equal Contribution.

indent Traditionally, domain experts analyze XRD samples by examining their peak characteristics such as the peak position, intensity and peak width, using their domain knowledge and comparison against existing reference databases of composition-phase maps. Since the current high-throughput XRD experiment produces thousands of samples at once, the manual attribution of phases for each sample has become a formidable task. Recently, domain scientists have started leveraging standard clustering algorithms to reduce the sample space for manual labeling and validation, and obtain the potential composition-phase diagram from a composition-spread experiment (Tatlier, 2011; Gilmore et al., 2004; Bunn et al., 2016). Such clustering techniques groups together XRD samples with similar peak characteristics, reducing the manual task of phase labeling from all samples to a small subset of samples in each group (phase region) (Hattrick-Simpers et al., 2016; Iwasaki et al., 2017). Once a

Jha, D., Narayanachari, K., Zhang, R., Keane, D., Liao, W., Choudhary, A., Chung, Y., Bedzyk, M. and Agrawal, A.
Enhancing Phase Mapping for High-throughput X-ray Diffraction Experiments using Fuzzy Clustering.
DOI: 10.5220/0010229905070514
In *Proceedings of the 10th International Conference on Pattern Recognition Applications and Methods (ICPRAM 2021)*, pages 507-514
ISBN: 978-989-758-486-2

small set of samples in each phase region is labeled, a supervised technique can be used to label the rest of the samples (Bunn et al., 2016). Recently, Park et al. (Park et al., 2017) used a CNN to classify the computed XRD patterns from ICSD (Bergerhoff et al., 1983) since it is impossible to get a large collection of labeled experimental samples (Park et al., 2017). Jha et al. (Jha et al., 2019) designed a peak area detection network for classification of phases from 2D warped XRD patterns using an experimental dataset containing 177 samples. The application of supervised learning for the analysis of XRD samples from experiments has been limited because it is impossible to obtain a large sample of experimental XRD samples with their phase labels. The primary focus of our work is to leverage machine learning techniques to help reduce the effort required by domain experts for XRD analysis and phase indexing.

A key aspect of XRD analysis is that composition-phase diagrams are composed of not only pure phases but also contain their mixed phases. A pure phase represents a single crystal structure for a given materials composition. A mixed phase represents a combination of multiple pure phases and hence, mixture of more than one crystal structure for the given material composition. A composition-phase diagram represents the phase (crystal structure) at different compositions for a given material alloy system. Composition-phase diagrams are generally composed of multiple pure phases, and their mixed phases. The current practice of using clustering techniques is based on hard clustering which assigns each sample to a single cluster (phase). A key issue with the current practice of directly applying hard clustering techniques on the 1D XRD patterns by domain scientists for phase clustering is that although a mixed phase is a composition of multiple pure phases, they treat them as separate cluster, independent of the pure phase clusters. Such treatment of pure phase and mixed phase as separate clusters leads to incorrect potential phase maps which complicates further manual analysis required during phase indexing. Here, our goal is to provide a method for phase clustering of XRD samples that can automatically handle the mixed phases by allowing multiple membership for those samples to their respective constituent pure phases.

In this paper, we present a novel clustering approach for high-throughput XRD experiments by leveraging a fuzzy clustering technique which can automatically handle the mixed phases by allowing multiple pure phase membership, and hence, significantly enhance the quality of potential composition-phase diagrams and reduce the manual efforts involved in next steps of phase labeling and validation. First, we apply a fuzzy c-means clustering algorithm to generate the initial composition-phase diagram and initial pure phase representations. Note that there exists several approaches for soft clustering (Baraldi and Blonda, 1999; Peters et al., 2013), here, we chose the prominent fuzzy c-means clustering algorithm for better interpretation and suitability to our clustering task. Next, the initial pure phase representations are analyzed using hierarchical clustering to find their similarity in peak characteristics by leveraging domain knowledge, and the similar initial pure phases are combined to obtain the final composition-phase diagram for the given composition-spread experiment. The proposed method is evaluated on XRD samples from two high-throughput XRD composition-spread experiments for the ternary alloy systems of Co-Ni-Ta and Co-Ti-Na (containing 1955 and 1533 samples respectively). The composition-phase diagrams obtained using our approach are in good agreement with manually computed ground truth composition-phase diagrams for the two ternary systems. Our results are verified by domain scientists and demonstrates significant advantage over current practice of hard clustering, drastically simplifying and reducing the manual efforts.

2 BACKGROUND

X-ray diffraction is an atomic scale probing technique to determine the crystal structure of materials for understanding their composition-structure-property relationships (Klug and Alexander, 1974; Moore and Reynolds, 1989; Bish and Post, 1989; Cullity, 1978; Woolfson and Woolfson, 1997). During an X-ray diffraction experiment, the crystal structure in the material causes the beam of incident X-rays to diffract into many specific directions; a 3D image representing the density of electrons in the crystal can be constructed by measuring the angles and intensities of the diffracted intensity patterns.

An X-ray pattern is basically a plot of the intensity of X-rays scattered at different angles by a materials sample, as measured by a 2D detector, with each pixel measuring the number of incident X-ray photons.The XRD pattern from a material composed of periodic atomic structures is composed of multiple sharp spots known as Bragg diffraction peaks; the positions and intensities of these peaks determine the phase of the materials - the specific chemistry and atomic arrangement. For instance, quartz, cristobalite and glass are all different phases of SiO_2; they are chemically identical but the atoms are arranged differently, the XRD pattern is distinct for each phase. A composition-

phase map represents the physical conditions at which thermodynamically distinct phases occur and coexist. The constituent phases in the composition-phase map represent the different crystal lattice structures for varying material composition. The clustered data is represented on a ternary composition-phase diagram as a function of atomic fractions. The phase clustering results can also be plotted for visualization and further analysis using a circular plot which maps the phase and the X-Y coordinates of the wafer used during XRD experiment.

3 PROPOSED APPROACH

The proposed method for the phase mapping of high-throughput XRD experiments consists of two main steps. First, we leverage a fuzzy c-means clustering technique on the XRD patterns to generate an initial potential composition-phase diagram and initial pure phase representations. Next, we analyze these pure phase representations using hierarchical clustering, and combine similar initial pure phases to obtain the final composition-phase diagram.

The first step in the proposed approach for XRD analysis is to perform an initial fuzzy phase clustering. There exist multiple soft clustering algorithms for fuzzy clustering (Baraldi and Blonda, 1999; Peters et al., 2013), here chose the fuzzy c-means clustering algorithm from Bezdek (Bezdek, 1981) for its simplicity of application to our task and better interpretation.

Let's define the XRD dataset as

$$X = \mathbf{x}_1, \mathbf{x}_2, ..., \mathbf{x}_n \tag{1}$$

such that each sample is a vector of m intensity values represented by:

$$\mathbf{x}_i = x_{i1}, x_{i2}, ..., x_{im} \tag{2}$$

Fuzzy c-means (FCM) clustering algorithm creates c fuzzy partitions by optimizing the following objective function:

$$J_m(U, \mathbf{v}) = \sum_{k=1}^{n} \sum_{i=1}^{c} (\mu_{ik})^{m'} (d_{ik})^2 \tag{3}$$

where

$$d_{ik} = d(\mathbf{x_k} - \mathbf{v_i}) = \left[\sum_{j=1}^{m} (x_{kj} - v_{ij})^2 \right]^{1/2} \tag{4}$$

represents the distance between the i^{th} cluster center $\mathbf{v}_i$ and the k^{th} XRD sample using Euclidean distance, μ_{ik} is the membership of the k^{th} sample in the i^{th} cluster such that

$$\sum_{i=1}^{c} \mu_{ik} = 1 \text{ for all } k = 1, 2, ..., n \tag{5}$$

where $\mathbf{v}_i$ is the i^{th} cluster center, which represents the pure phase using a vector of m intensity values in the form $\mathbf{v}_i = v_{i1}, v_{i2}, ..., v_{im}$ computed as:

$$v_{ij} = \frac{\sum_{k=1}^{n} \mu_{ik}^{m'} \cdot x_{kj}}{\sum_{k=1}^{n} \mu_{ik}^{m'}} \tag{6}$$

where U is the partition matrix with c rows and n columns formed by μ_{ik}, represents the fuzzy membership of an XRD sample to the c pure phase clusters, m' is the weighting parameter that controls the amount of fuzziness in the phase clustering process.

The range for the membership exponent is $m' \varepsilon [1, \infty)$. For the case of $m' = 1$, the distance norm is the original distance metric used (Euclidean by default) and the algorithm approaches a hard c-means algorithm, where each XRD sample would belong to a single cluster. This objective function is optimized to get the best solution within a pre-specified level of accuracy ε using the iterative optimization.

The fuzziness in the clustering is measured by computing the fuzzy partition coefficient (FPC) as follows:

$$F_c U = \frac{tr(U * U^T)}{n} \tag{7}$$

where U is the fuzzy partition matrix representing the membership of each data point to different clusters, n is the number of samples in our dataset, and the operation $*$ represents matrix multiplication. This partition coefficient has some special properties. If $F_c U = 1/c$, it means the clustering is completely ambiguous, while if $F_c U = 1$, it means hard clustering, i.e., each data sample belongs to a single cluster. Generally, the number of pure phases in a phase diagram for a given composition space is not very large. A high value of membership (ideally 1) represents the sample having a pure phase, while a lower value of membership represents a mixed phase. The cluster centers from FCM provide the pure phase representation for each pure phase in the potential phase diagram for the given composition space.

The initial composition-phase diagram from fuzzy clustering can be composed of multiple overlapping clusters due to the presence of multiple initial pure phases with similar representations. Therefore, the next step is to combine together similar initial pure phases to obtain the final composition-phase diagram. To accomplish the combination of similar initial pure phases from fuzzy clustering step, we leverage hierarchical clustering with its corresponding dendogram to visually analyze the initial pure phase representations before combining them.

4 EXPERIMENTAL RESULTS

We present the experimental results using the proposed approach for phase mapping of high-throughput XRD experiments in this section. First, we discuss the XRD datasets used for evaluation. Next, we present our experimental results, followed by comparison against current practice of using hard clustering algorithms of hierarchical clustering and k-means clustering. All the experimental evaluations are implemented using Python.

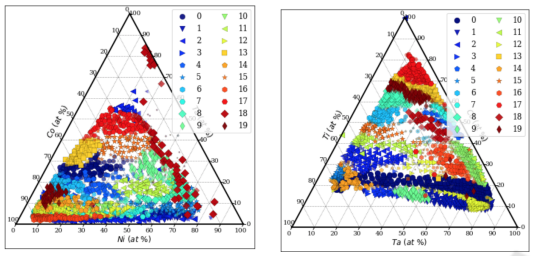

(a) Co-Ni-Ta (b) Co-Ti-Ta

Figure 1: Initial composition-phase diagram (phase clustering output) using FCM algorithm. These ternary plots show both pure phases and mixed phases, the membership of a sample to a cluster is represented using the opaqueness and size of marker.

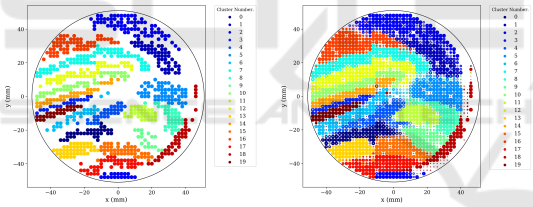

(a) Co-Ni-Ta (samples with memb $>$ .95) (b) Co-Ni-Ta (all samples)

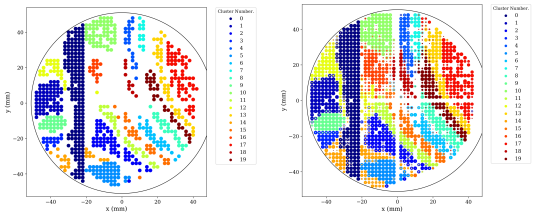

(c) Co-Ti-Ta (samples with memb $>$ .95) (d) Co-Ti-Ta (all samples)

Figure 2: Circular plots representing the phase clustering results using FCM algorithm. The left subplots only show samples having membership $>$ 0.95, which should represent the samples with pure phases, the right subplots also include the ones with mixed phases. the membership of a sample to a cluster is represented using the opaqueness and size of marker. For samples with mixed phases, the marker is more transparent with smaller size.

4.1 Datasets

The dataset used in this study is collected from two high-throughput composition-spread using concurrent X-ray diffraction (XRD) and X-ray fluorescence (XRF) experiment for the composition space of Cobalt, Nickel and Tantalum (Co-Ni-Ta) and the composition space of Cobalt, Titanium and Tantalum (Co-Ti-Ta). The data acquisition experiments were carried out using a customized setup at beam-line 5BMC of Advanced Photon Source (APS) in Argonne National Lab. The collected XRD data is used in this study for phase mapping analysis. The XRF data is used to calculate atomic ratios. The 2D XRD diffraction patterns collected from the X-ray detector were converted to 1D by circular averaging the counts to reduce the effect of texturing on the XRD data. The 1D XRD data is further processed to account for the incident beam brightness change across the samples and for the background removal using 2nd order polynomial fit to the background. The angular position 2θ of the diffracted X-ray peak is converted to Q-values. The Q-values are independent of X-ray energy and directly related to the inverse d-spacing on the planes diffracting the X-rays. The Co-Ni-Ta dataset contains $1,859$ samples with intensities at 499 Q-values in the range of $[1.0, 4.2]$ from the high-throughput X-ray diffraction experiment. The Co-Ti-Ta dataset contain the values of intensities at $1,450$ Q-values in the range of $[1.0, 4.3]$ for $1,533$ samples from the high-throughput X-ray diffraction experiment. The dataset also contains the composition of each sample along with the X-Y position on the wafer used during experimentation; the composition is used to plot the ternary plot and the X-Y position is used for the circular plot for XRD analysis.

4.2 Fuzzy Clustering

The first step in the proposed approach is to apply the FCM algorithm to generate an initial composition-phase diagram and initial pure phase representations. For this, we leveraged the FCM algorithm implementation from SciKit-Fuzzy (Warner,). It takes the *error* (stopping criterion used to stop early if the norm of change in membership is less than the provided value), m (array exponentiation applied to the membership function at each iteration), $maxiter$ (maximum number of iterations allowed), *init* (the initialization for fuzzy c-partitioned matrix), along with the data and desired number of clusters as inputs, and returns the cluster centers, final fuzzy c-partitioned matrix and FPC as the output. After experimenting with different combinations of the input param-

eters for both datasets, we present the best results obtained using the following input parameters for both datasets: 0.01 for *error*, 1.13 for *m*, *euclidean* as the *distance_metric*. For *maxiter*, we used 500 for Co-Ni-Ta and 10,000 for Co-Ti-Ta, they worked best. We experimented using number of clusters in the range of [1,50) for the FCM algorithm. Since the expected number of clusters is in the range of [10,20] for both datasets, we select the clustering results with 20 clusters for both datasets as fuzziness was highest for this case, so that we do not miss any pure phases which may lead to incorrect composition-phase diagram. Next, we analyzed the membership of each pure phase (cluster) by their sample count. Ideally, a sample belonging to a pure phase should have a perfect membership value of 1 to that pure phase (cluster). In practice, we looked at the sample counts with membership value $>$0.9 for each pure phase; the minimum sample count for each cluster was 20.

There exists two approaches for visualizing the clustering results of samples from a high-throughput XRD experiment- ternary plot and circular plot. A ternary composition-phase diagram represents the phase for each sample with respect to its material composition as shown in Figure 1. From Figure 1, we observe that most clusters are well-separated from each other, which represents clear phase regions. The distinct phase regions (clusters) in the ternary plot represent distinct pure phases where each pure phase represents a particular arrangement of atoms, resulting in a particular crystal structure for the material compositions in that phase region. The size and opaqueness of markers used for plotting represents the membership to a particular phase; smaller markers representing samples having multiple membership (fuzzy membership), hence, mixed phase regions (which can not be handled by the hard clustering algorithms used in current practice of phase clustering). Since a mixed phase is a combination of multiple pure phases, the composition region representing mixed phases in the ternary plot have multiple types of crystal structures for the given material composition. A circular plot maps the phase clustering output with the X-Y coordinates of the wafer used during XRD experiment. Left subplots of Figure 2 only shows the samples with pure phases while the right subplots include samples having mixed phase as well. Comparing between the left and right subplots, we can observe that the mixed phase region (empty in the left subplots) generally lies between its constituent pure phases. The marker size and opaqueness having similar representation as before; smaller dots represent the samples with mixed phases (having membership to multiple pure phases). A mixed phase can be a combination of any number of constituent pure phases present in the phase diagram. Since there are 20 initial pure phases, there exist several mixed phases in the composition phase diagram, having varying degree of membership to their constituent pure phases.

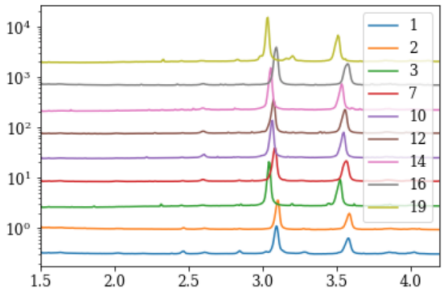

Figure 3: A candidate set of similar initial pure phases from applying FCM algorithm on the Co-Ni-Ta dataset that can be merged together to obtain the final composition-phase diagram.

4.3 Merging Procedure

After analyzing the initial pure phase representations, we observe that there are multiple sets of similar initial pure phases which should belong together. Figure 3 demonstrates one such candidate set containing nine initial pure phases similar to each other; they have similar representations, suggesting that they belong to same phase and have same underlying crystal structure. For the merging procedure, first we obtain the dendogram by applying hierarchical clustering on the initial pure phase representations. Next, we visualized and analyzed each set of similar initial pure phases to decide which ones to combine, such as the set of initial pure phases for Co-Ni-Ta shown in Figure 3. We finally merged together sets of initial pure phase representations to obtain the pure phases in the final composition-phase diagrams as illustrated in Figure 4. There are 9 final pure phases for both composition spaces in our study; they have obvious difference in their peak characteristics which represents different underlying crystal structures for their corresponding samples. We updated the membership for each sample to obtain the final composition-phase maps shown in Figure 5. Comparison between the shape and location of phase regions in the composition phase diagrams using the proposed method and the manually computed phase diagrams by domain experts in our team shows that they are in good agreement with each other and concur with the expectations of domain scientists.

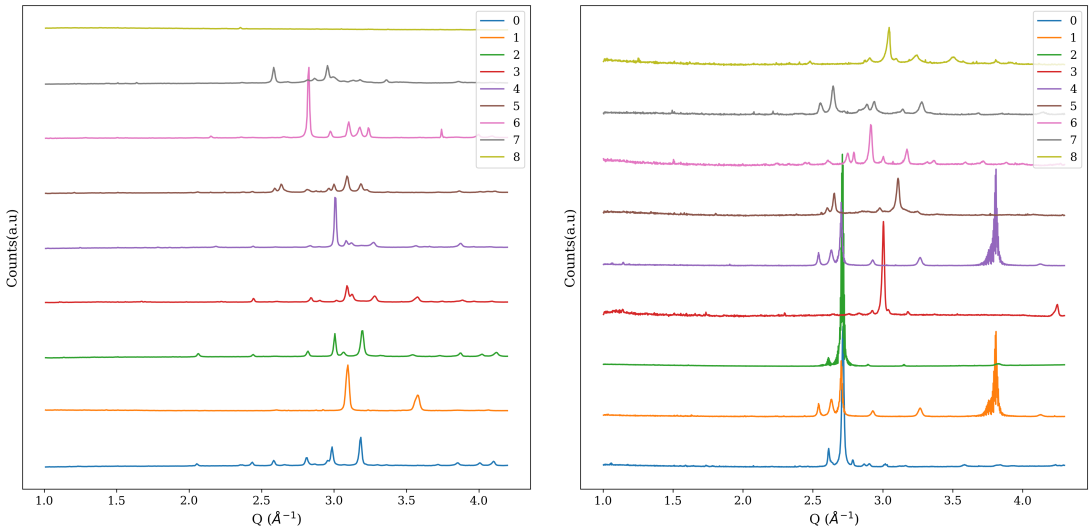

(a) Co-Ni-Ta (b) Co-Ti-Ta

Figure 4: Final pure phase representations after merging similar initial pure phases. The final pure phase representations are significantly different from each other which illustrates the efficiency of the proposed approach.

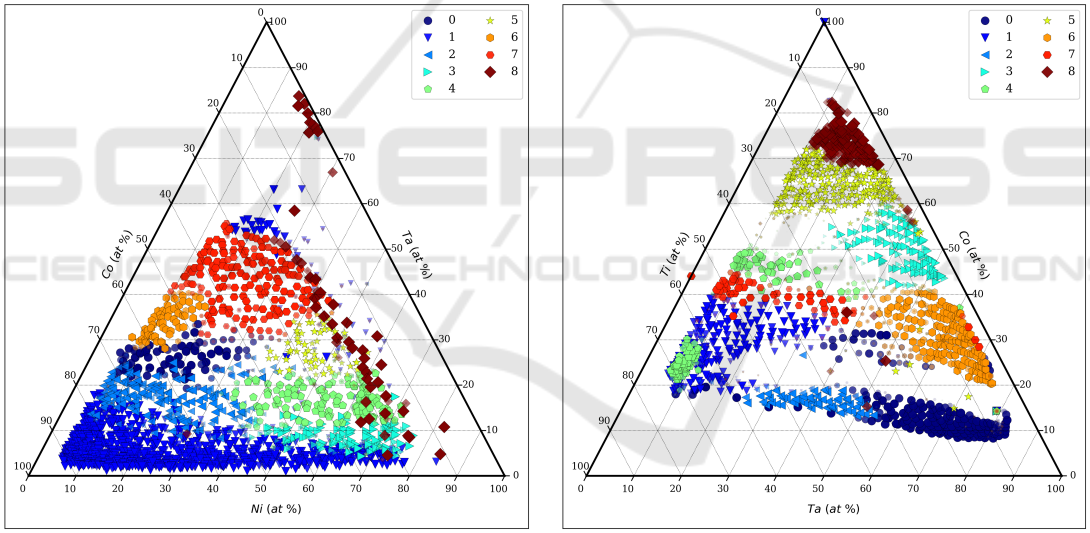

(a) Co-Ni-Ta (b) Co-Ti-Ta

Figure 5: Final composition-phase diagram using proposed approach. There are 9 final pure phases for both ternary systems.

4.4 Comparison against Current Approaches of Hard Clustering

Next, we compared the proposed approach against the current practice of directly using hard clustering algorithms on the 1D XRD patterns (Bunn et al., 2016; Hattrick-Simpers et al., 2016; Iwasaki et al., 2017); these include hierarchical clustering and k-means clustering. For hierarchical clustering, we experimented with all the available distance metrics in SciPy (Jones et al., 01) such as cosine, correlation, braycurtis, mahalanobis and euclidean. For k-means clustering, we experimented with values of k in the range of [5,20].

Figure 6 demonstrates one of the best phase clustering results using hierarchical clustering on the two datasets. There are a large number of clusters in both cases- 64 clusters for Co-Ni-Ta and 91 clusters for Co-Ti-Ta. Note that we experimented using all the exhausting list of values for different metrics and parameters for hierarchical clustering, and Figure 6 represents one of the best results. From the composition-phase diagrams, we observe that there are large clus-

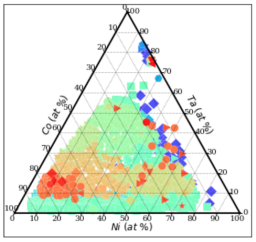

(a) Co-Ni-Ta, Hierarchical Clustering

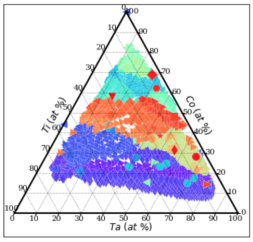

(b) Co-Ti-Ta, Hierarchical Clustering

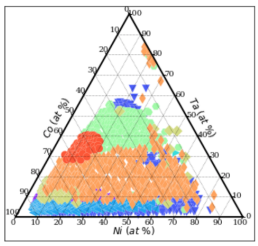

(c) Co-Ni-Ta, K-means clustering

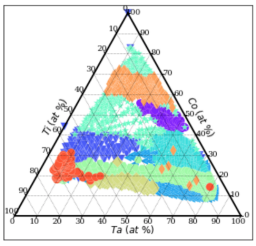

(d) Co-Ti-Ta, K-means clustering

Figure 6: Composition-phase diagrams using current practice of directly applying hierarchical clustering and k-means clustering. For hierarchical clustering, correlation is used as the distance metric in both case, the *hc_param* is 0.48828 for both cases; there are 64 clusters for Co-Ni-Ta and 91 clusters for Co-Ti-Ta. For k-means clustering, we present clustering results from $k = 9$ here, since there are 9 phases in the final phase diagram expected by domain experts.

ter regions, but the boundary between different phase regions is not clear in either case. We observe more clear clusters in the case of k-means clustering as shown in Figure 6, but they do no agree with the expectation of domain experts. If we compare the results of k-means against hierarchical clustering, we can clearly observe that composition phase diagram from hierarchical clustering is closer to the domain expectation. If we compare these hard clusters against the results using phase clustering results obtained using the proposed technique, we find that multiple pure phases from the proposed technique are clustered together in the phase clustering output using hierarchical clustering. If the clustering technique cannot handle the difference between pure phases and mixed phases, the resulting phase diagram can be incorrect. Since a mixed phase region is generally located between its constituent pure phases, the distinction is not clear if the clustering does not consider this property. In contrast, there is a clear distinction between the pure phase regions output by the proposed method; the mixed phases are found to be well located between their constituent phases. This illustrates the benefit of using the proposed phase mapping approach for high-throughput XRD experiments over the current practice of using hard clustering techniques which cannot distinguish between pure phases and mixed phases.

5 CONCLUSIONS AND FUTURE WORKS

In this paper, we presented a novel approach to enhance the phase mapping of high-throughput experiment by combining the fuzzy c-means clustering algorithm with effortless manual analysis by domain experts using hierarchical clustering. The proposed phase mapping approach is evaluated using samples from high-throughput experiment for the composition space of two ternary alloys- Co-Ni-Ta and Co-Ti-Ta. The results obtained using current clustering techniques illustrate that hard clustering algorithms are not suitable for analysis of 1D XRD patterns. Even though distance metrics which are resilient to peak shifting, such as dynamic time warping (DTW) and earth mover's distance (EMD), they still do not work for 1D XRD patterns. On the other hand, we demonstrated that we can leverage together a fuzzy clustering algorithm with the well known euclidean metric, along with traditional hard clustering algorithm (hierarchical clustering) with a little manual analysis by domain experts to produce composition phase diagram that closely resemble the manually computed phase diagram by domain scientists. This illustrates that handling the mixed phases is a key issue in performing phase clustering analysis for 1D XRD patterns. The results in this work are compared against the potential manually computed phase diagrams in past literature and validated by domain experts. For both Co-Ni-Ta and Co-Ti-Ta composition spaces, there are nine pure phases present in the manually computed phase diagram and hence, expected by domain experts. Although the presented approach requires a small amount of manual analysis of the initial pure phase representations for merging in the second step, we expect it to significantly reduce the existing manual efforts required in the phase mapping of large volume of samples coming from high-throughput XRD experiments. The code implementation of the proposed approach is available at `https://github.com/dipendra009/FuzzyClustering`. We plan to work towards automating the overall process in the future and release resulting software for domain scientists for the analysis of their high-throughput XRD datasets.

ACKNOWLEDGMENT

This work was performed under the following financial assistance award 70NANB14H012 and 70NANB19H005 from U.S. Department of Commerce, National Institute of Standards and Technology as part of the Center for Hierarchical Materials Design (CHiMaD), DND-CAT located at Sector 5 of the Advanced Photon Source (APS) at Argonne National Lab supported by DOE under Contract No. DE-AC02-06CH11357, the MRSEC program of the National Science Foundation (DMR-1720139), and the Soft and Hybrid Nanotechnology Experimental (SHyNE) Resource (NSF NNCI-1542205). Partial support is also acknowledged from DOE awards DE-SC0014330, DE-SC0019358.

REFERENCES

Baraldi, A. and Blonda, P. (1999). A survey of fuzzy clustering algorithms for pattern recognition. ii. *IEEE Transactions on Systems, Man, and Cybernetics, Part B (Cybernetics)*, 29(6):786–801.

Bergerhoff, G., Hundt, R., Sievers, R., and Brown, I. (1983). The inorganic crystal structure data base. *Journal of chemical information and computer sciences*, 23(2):66–69.

Bezdek, J. C. (1981). Objective function clustering. In *Pattern recognition with fuzzy objective function algorithms*, pages 43–93. Springer.

Bish, D. L. and Post, J. E. (1989). *Modern powder diffraction*, volume 20. Mineralogical Society of America Washington, DC.

Bunn, J. K., Hu, J., and Hattrick-Simpers, J. R. (2016). Semi-supervised approach to phase identification from combinatorial sample diffraction patterns. *JOM*, 68(8):2116–2125.

Chung, J.-S. and Ice, G. E. (1999). Automated indexing for texture and strain measurement with broad-bandpass x-ray microbeams. *Journal of applied physics*, 86(9):5249–5255.

Cullity, B. (1978). Elements of xrd diffraction, addition-wesley. *Reading, MA*.

Gilmore, C. J., Barr, G., and Paisley, J. (2004). High-throughput powder diffraction. i. a new approach to qualitative and quantitative powder diffraction pattern analysis using full pattern profiles. *Journal of applied crystallography*, 37(2):231–242.

Hattrick-Simpers, J. R., Gregoire, J. M., and Kusne, A. G. (2016). Perspective: Composition–structure–property mapping in high-throughput experiments: Turning data into knowledge. *APL Materials*, 4(5):053211.

Iwasaki, Y., Kusne, A. G., and Takeuchi, I. (2017). Comparison of dissimilarity measures for cluster analysis of x-ray diffraction data from combinatorial libraries. *npj Computational Materials*, 3(1):4.

Jha, D., Kusne, A. G., Al-Bahrani, R., Nguyen, N., Liao, W.-k., Choudhary, A., and Agrawal, A. (2019). Peak area detection network for directly learning phase regions from raw x-ray diffraction patterns. In *2019 International Joint Conference on Neural Networks (IJCNN)*, pages 1–8. IEEE.

Jones, E., Oliphant, T., Peterson, P., et al. (2001–). SciPy: Open source scientific tools for Python. [Online; accessed ¡today¿].

Klug, H. P. and Alexander, L. E. (1974). X-ray diffraction procedures: for polycrystalline and amorphous materials. *X-Ray Diffraction Procedures: For Polycrystalline and Amorphous Materials, 2nd Edition, by Harold P. Klug, Leroy E. Alexander, pp. 992. ISBN 0-471-49369-4. Wiley-VCH, May 1974.*, page 992.

Moore, D. M. and Reynolds, R. C. (1989). *X-ray Diffraction and the Identification and Analysis of Clay Minerals*, volume 322. Oxford university press Oxford.

Park, W. B., Chung, J., Jung, J., Sohn, K., Singh, S. P., Pyo, M., Shin, N., and Sohn, K.-S. (2017). Classification of crystal structure using a convolutional neural network. *IUCrJ*, 4(4):486–494.

Peters, G., Crespo, F., Lingras, P., and Weber, R. (2013). Soft clustering–fuzzy and rough approaches and their extensions and derivatives. *International Journal of Approximate Reasoning*, 54(2):307–322.

Tatlier, M. (2011). Artificial neural network methods for the prediction of framework crystal structures of zeolites from xrd data. *Neural Computing and Applications*, 20(3):365–371.

Warner, J. Scikit-fuzzy: A fuzzy logic toolbox for scipy.

Woolfson, M. M. and Woolfson, M. M. (1997). *An introduction to X-ray crystallography*. Cambridge University Press.